ELSEVIER

Neurocomputing 32–33 (2000) 213–218

NEUROCOMPUTING

www.elsevier.com/locate/neucom

Are inhibitory synaptic conductances on thalamic relay neurons inhomogeneous? Are synapses from individual afferents clustered?

M. Neubig*, A. Destexhe[1]

Laboratoire de Neurophysiologie, Faculté de Médecine, Université Laval, Québec, Canada G1K 7P4

Accepted 11 January 2000

Abstract

Standard and dynamic current clamps were used to emulate dendritic GABA-Aergic postsynaptic currents (IPSCs) in a reconstructed thalamic relay neuron. The variability of somatically recorded single events was an order of magnitude smaller than reported in experimental work, suggesting that experimentally observed variability of miniature IPSCs reflects variable synaptic strength rather than filtering. Additionally, to evoke physiologic unitary-IPSCs at 0.8 probability-of-release, it was necessary to partially cluster synapses. This induced nonlinear summation — bringing unitary amplitudes down to the observed range. We conclude that synaptic strength is inhomogeneous and that inhibitory afferents might form synapses in clusters.

Keywords: Postsynaptic potentials; Inhibition; Thalamus; Dendrites

1. Introduction

The long-standing interest in the functional importance of the input to thalamic nuclei from the GABAergic thalamic reticular nucleus has led to several recent studies which report new data on the chloride-dependent component of inhibitory postsynaptic currents (IPSCs). In particular, new data has been gathered on miniature IPSCs and unitary IPSCs [2,5,6,14].

* Corresponding address: Salk Institute – CNL, 10010 N. Torrey Pines Road, La Jolla, CA 92037, USA. Tel.: + 858-453-4100X1124; fax: + 1-858-587-0417.

E-mail address: neubig@salk.edu (M. Neubig).

[1] Present address: UNIC, Institut de Neurobiologie Alfred Fessard, CNRS, Avenue de la Terrasse, 91128 Gif-sur-Yvette, France.

0925-2312/00/$ - see front matter
PII: S0925-2312(00)00166-1

Putatively, miniature IPSCS (mIPSCs) arise from exocytosis of single vesicles of transmitter, while unitary IPSCs (uIPSCs) stem from the firing of single presynaptic cells, e.g. during paired recordings.

The degree to which dendritic filtering, or, alternatively, inhomogeneity of synaptic strength, contributes to the observed variability of mIPSC data has not been assessed for thalamic relay cells. Also, the distribution of synapses made by individual reticularis neurons on individual relay neurons is unknown.

To address these questions, synaptic currents were emulated by dendritic current clamps (standard and dynamic) in a series of computational experiments run on a 1417-compartment reconstructed thalamic relay neuron. Recordings of mIPSCs and uIPSCs were made under conditions analogous to somatic voltage clamp and reversed chloride potential.

2. Methods

In a previous study [4], a thalamic relay neuron from the ventrobasal nucleus of a p10 rat had been recorded in whole cell mode with cesium-free solutions. It was digitized into 1201 points using 80 μm resections of the original 400 μm slice. The mean distance between points was 6.0 ± 2.8 μm. This reconstruction has been used in our previous computational studies. [3,8–11].

Two additional corrections were made here. Twenty-seven branches which were minute and totaled 25 μm^2 have been removed because they were created to accommodate the digitization algorithm. Also, the somatic membrane has been reduced by 11% to 2870 μm^2 to exclude the ficticious membrane occluding the dendritic trunks.

Each of the remaining 178 branches was subdivided based on electrotonic length. A target of $0.01\,\lambda$ established 1416 segments with a mean anatomical length of 5.0 ± 0.7 μm. Trials were run under Linux on a Pentium II machine using NEURON with a fixed time-step of 25 μs.

Refining the spatial and temporal discritization by a factor of 2 resulted in a less than 0.1% change in mIPSC amplitude and phase. This indicates that the structure revealed by Fig. 1 data, particularly the left histogram, is a signature of the arbor, not noise.

In other control simulations, a low threshold calcium current [1], which is abundant in this cell type, altered mIPSCs by less than 0.5%, prompting its further exclusion.

3. Results

3.1. Miniature IPSCs

Injections of a 14 pA synaptic current-waveform (Fig. 1A, inset) appeared as 11.1–12.7 pA events in the recording traces (Fig. 1A). The median over all regions of the arbor was 12.3 pA ($n = 1417$, vertical bars, Fig. 1A). The median rise time

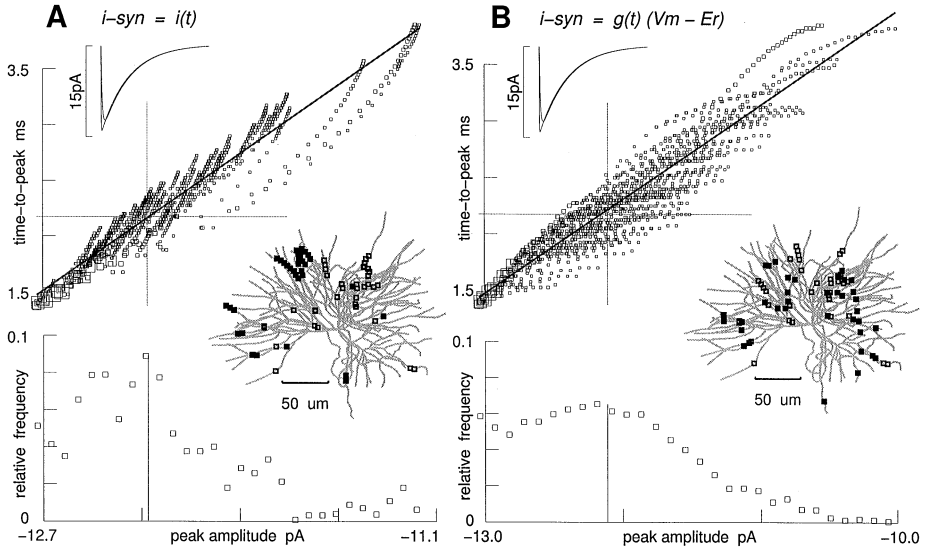

Fig. 1. Miniature IPSC variability due to filtering. Dendritic synaptic currents were emulated by (A) injection of a current-waveform or by (B) dynamic current clamp. These events were recorded through a somatic voltage clamp. Holding potential was 46 mV negative to the dynamic clamp's reversal potential; uncompensated series resistance was 1 MΩ; 21°C.

INSET CURRENT TRACES: 55 ms 14 pA synaptic current timecourses are superimposed with median mIPSCs. SCATTER PLOTS: peak amplitudes vs. time-to-peaks of the events as seen through a somatic voltage clamp. Data for emulations at each of the 1417 compartments is given. Area of squares is proportional to area ascribed to the compartment. WEIGHTED LEAST-SQUARES LINES: $y = ax + b$, A: $a = 1.54$ ms/pA $b = 21.0$ ms; B: $a = 0.84$ ms/pA $b = 12.4$ ms. CROSSHAIRS: medians. RELATIVE HISTOGRAMS: comprise data for peak amplitudes of recordings; compartments weighted for local inhibitory synapse density. MORPHOLOGY PLOTS: sites yielding values closest to median. FILLED SQUARES: 36 emulation sites whose mIPSCs peak amplitudes were closest to the median. OPEN SQUARES: 36 median time-to-peak sites. The arbor has been FLATTENED to the viewing plane, as opposed to projected, with a length and orientation preserving algorithm: appearant distance is actual. Scale bar applies to any direction. Dendrite diameter is not shown.

EQUATIONS: A: i-syn = pk*$F(t)$/fct, where $F(t) = d + \exp[-(t + s - \text{on})/(f/q)] - \exp[-(t + s - \text{on})/(r/q)]$ where $pk = 14$ {pA, t = time, on = trigger time, $f = 13.9$ ms, q: Q10 = 2.1, $r = 0.1$ ms, fct = Max($F(t)$), "d" shifted the timecourse downward by 2% so that i-syn became zero after a finite interval (55 ms @ 21°C), while "s" shifted it leftward to compensate; B: $g(t)$ = pk*$F(t)$/fct where pk = 312e-6 S/cm^2. INPUT RESISTANCE, ETC: R-input of the 24 236 sq micron cell was 398 MΩ with T-current, corresponding to the cesium-loaded condition of the cited experiments. Leak conductance = 13e-6S/cm^2, axial resistivity = 200 Ω cm, capacitance = 1.0 μF/cm^2.

(10–90%) and time-to-peak were 0.98 and 2.18 ms (horizontal bars, Fig. 1A). The former ranged from 0.45 to 1.95 ms.

(Data reported herein have been weighted to reflect the number of inhibitory synapses represented by each compartment. Inhibitory synapses occur throughout the arbor [7,13].)

Impositions of a dynamic clamp with a 312 pS peak conductance appeared as 10.0–13.0 pA events (median 12.1 pA, Fig. 1B). The medians and ranges for the

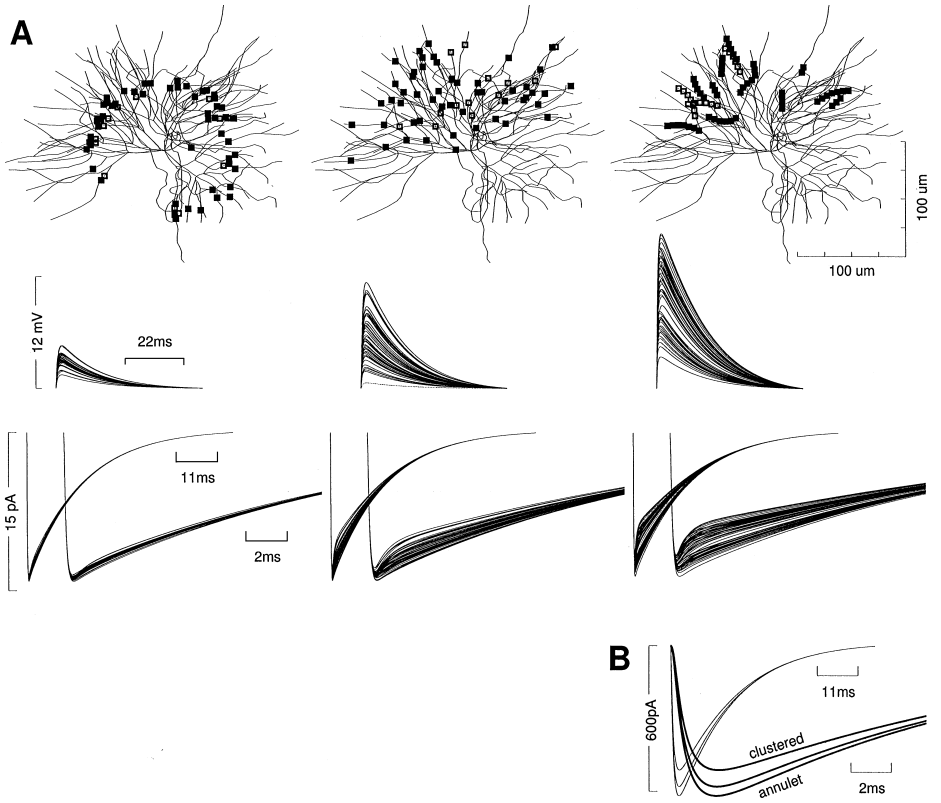

Fig. 2. Clustering of synapses on thalamic dendrites. Escape voltages are enhanced when unitary synapses are clustered. This reduces individual synaptic currents and leads to physiologic uIPSCs. (A) Three distributions of inhibitory synapses. In each case $n = 66$, which corresponds to numbers typically observed as arising from single afferents (11,60,62,69,69: see discussion). LEFT: sparsely distributed sites representing all 11 trees. No two are closer than 50 μm, all are 67 μm remote, which is the median distance from the soma of dendritic membrane. MIDDLE: sparsely distributed sites representing two trees. No two are closer than 25 μm, but are random otherwise. RIGHT: clustered sites, same two trees as before, grouped into 11 clusters with 20 μm radii. No two clusters are closer than 100 μm, but are random otherwise. FILLED SQUARES: $n = 53$ emulated synapses. OPEN SQUARES: $n = 13$ non-firing synapses. VOLTAGE TRACES: escape voltages were recorded numerically at each emulation site and superimposed here. Their amplitude reflects the quality of space clamp created by the somatic voltage clamp. Transients are depolarizations since a reversed chloride potential has been used. CURRENT TRACES: Synaptic currents generated by multiple dynamic current clamps, shown at two time scales. i-syn = pk*$F(T)$/fct* (Vm-Er), where $F(T)$/fct is a dual exponential conductance time course, Vm = transmembrane potential, Er = reversed chloride equilibrium potential, see Fig. 1. (B) uIPSCS (somatic voltage clamp recordings) on two time scales; recordings for all three cases are superimposed. The clustered uIPSC is at the upper range of values in the literature (56–514 pA), implying that even denser clustering is required for median physiologic uIPSCs (and/or higher failure-rate); see Discussion.

temporal statistics were identical to those taken under the current-waveform paradigm.

These results may be compared to recently published data: mIPSC peak amplitudes are 12.2 ± 2.6 pA [2] with a 2.0 ± 0.3 ms time-to-peak [6], and a 13.9 ± 1.4 ms decay time constant [6]. The correspondence is not coincidental, as this experimental data was used explicitly to constrain our emulation equations (see caption of Fig. 1).

3.2. Unitary IPSCs

A sparse selection was made of 53 sites of median remoteness which also satisfied a 50 μm nearest-neighbour criteria (Fig. 2A-Left). Simultaneous activation of dynamic clamps at these sites appeared as a single 619 pA event at the soma (Fig. 2B). The actual net synaptic current generated by the multiple dynamic clamps was 729 pA (avg: 13.75), which is comparable to the sum under the single activation paradigm (735 pA).

(Data not shown: Another set of 53 sites were selected which satisfied a 50 μm nearest-neighbour criteria, and were scattered throughout the arbor. Their uIPSCs and net currents were 602 and 729 pA.)

Another set of 53 sites satisfying a 25 μm nearest-neighbour criteria were selected from two trees (Fig. 2A-Middle). When triggered simultaneously, these 53 currents appeared as a single 581 pA event in the current trace (Fig. 2B). In this case the synaptic currents totaled 710 pA (avg: 13.4), which is slightly diminished over the single activation paradigm (732 pA, avg: 13.8 pA). The 3% reduction is attributable to greater escape voltages: 2.1 vs. 5.8 mV (Fig. 2A).

A third set of 53 sites was selected, this time grouped into 11 clusters on the same two trees (Fig. 2A-Right). The cluster radius was 20 μm and the centres met a 100 μm nearest-neighbour criteria. In this case the recorded uIPSC reached 512 pA at its peak (Fig. 2B). Under the single activation paradigm, their average escape voltage and synaptic current were 2.5 mV and 13.8 pA (net: 731 pA), but when activated in-concert, the statistics rose/fell to 10.6 mV and 12.2 pA, (648 pA net), respectively.

4. Discussion

The amplitude distribution of GABA-Aergic mIPSCs in individual thalamic relay cells has been reported to range from 10 to 40 pA [2,6]. The source of this variability is unknown. Here, it has been shown that dendritic filtering can explain only 3 pA of that 30 pA spread. The remaining variability could be attributable to inhomogeneity in synaptic strengths, and/or to experimental uncertainties [12].

Single afferent reticularis neurons are thought to form 60–70 synapses per thalamic relay cell ($n = 5$ cells: 11,60,62,69,69, ferret slices) [5]. Their specific distribution is unknown. We have shown that if synaptic failure rates are 0–40% [2], then sparse distributions are untenable since they give rise to linearly summated uIPSCs whose amplitudes are beyond the reported range (56–514 pA, rat slices [2]).

For clustered synapses, however, we have shown that nonlinear summation occurs. In this case, reported anatomical data becomes consistent with reported electrophysiological data. The degree of clustering used here (5.5 synapses along 40 μm) led to uIPSCs in the upper physiologic range; middle range uIPSCs would dictate denser clustering and/or higher failure rates of synaptic transmission.

Acknowledgements

Research supported by the Medical Research Council of Canada (MT-13724) and a Fellowship to MN from Hydro-Quebec.

References

[1] D.A. Coulter, J.R. Huguenard, D.A. Prince, Calcium currents in rat thalamocortical relay neurons: kinetic properties of the transient, low-threshold current, J. Physiol. (London) 414 (1989) 587–604.
[2] C.L. Cox, J.R. Huguenard, D.A. Prince, Nucleus reticularis neurons mediate diverse inhibitory effects in the thalamus, Proc. Natl. Acad. Sci. USA 94 (1997) 8854–8859.
[3] A. Destexhe, M. Neubig, D. Ulrich, J. Huguenard, Dendritic low-threshold calcium currents in thalamic relay cells, J. Neurosci. 18 (10) (1998) 3574–3588.
[4] J.R. Huguenard, D.A. McCormick, Simulation of the currents involved in rhythmic oscillations in thalamic relay neurons, J. Neurophysiol. 68 (4) (1992) 1373–1383.
[5] U. Kim, M.V. Sanchez-Vives, D.A. McCormick, Functional dynamics of GABA-ergic inhibition in the thalamus, Science 278 (1997) 130–134.
[6] Y. LeFeuvre, D. Fricker, N. Leresche, $GABA_A$-receptor mediated IPSCs in rat thalamic sensory nuclei: patterns of discharge and tonic modulation by $GABA_B$ autoreceptors, J. Physiol. (London) 502 (1997) 91–104.
[7] X.B. Liu, C.N. Honda, E.G. Jones, Distribution of four types of synapse on physiologically identified relay neurons in the ventroposterior thalamic nucleus of the cat, J. Comp. Neurol. 352 (1995) 69–91.
[8] M. Neubig, A. Destexhe, Constraining morphological and biophysical parameters via minimization along behavioral metrics: low order compartmental models of thalamic relay neurons which preserve afferent synapse distribution, Soc. Neurosci. Abstr. 23 (1997) 230.3.
[9] M. Neubig, A. Destexhe, Dendritic calcium currents in thalamic relay cells, in: J.M. Bower (Ed.), Computational Neuroscience Trends in Research, Plenum Press, New York, 1998a, pp. 233–238.
[10] M. Neubig, A. Destexhe, LTS bursting and the subcellular localizations of T-type Ca^{2+} channels in thalamic relay neurons, Soc. Neurosci. Abstr. 24 (1998b) 407.10.
[11] M. Neubig, A. Destexhe, Low threshold calcium T-current IV curve geometry is alterable through the distribution of T-channels in thalamic relay neurons, Neurocomputing 26–27 (1999) 215–221.
[12] Z. Nusser, N. Hajos, P. Somogyi, I. Mody, Increased number of synaptic $GABA_A$ receptors underlies potentiation at hippocampal inhibitory synapses, Nature 395 (1998) 172–177.
[13] F. Sato, Y. Nakamura, Y. Shinoda, Serial electron microscopic reconstruction of axon terminals on physiologically identified thalamocortical neurons in the cat ventral lateral nucleus, J. Comput. Neurol. 388 (1997) 6133–6341.
[14] D. Ulrich, J.R. Huguenard, $GABA_A$-receptor mediated rebound burst firing and burst shunting in thalamus, J. Neurophysiol. 78 (1997) 1748–1751.